Electronic Supplementary Material (ESI) for Lab on a Chip.
This journal is © The Royal Society of Chemistry 2020
Electronic Supplementary Material (ESI) for Lab on a Chip.
This journal is © The Royal Society of Chemistry 2020

Supplementary Information

A liquid biopsy-guided drug release system for cancer theranostics: integrating rapid circulating tumor cell detection and precision tumor therapy

Chun-Miao Xu,[a] Man Tang,[a] Jiao Feng,[a] Hou-Fu Xia,[b] Ling-Ling Wu,[a] Dai-Wen Pang,[a] Gang Chen, [*b] Zhi-Ling Zhang[*a]

[a] Key Laboratory of Analytical Chemistry for Biology and Medicine (Ministry of Education), College of Chemistry and Molecular Sciences, Wuhan University, Wuhan 430072, P. R. China.

E-mail: zlzhang@whu.edu.cn

[b] The State Key Laboratory Breeding Base of Basic Science of Stomatology (Hubei-MOST) and Key Laboratory of Oral Biomedicine of Ministry of Education, School and Hospital of Stomatology, Wuhan University, Wuhan 430079, P. R. China.

[*]Co-corresponding authors:

Email: zlzhang@whu.edu.cn; Fax: 0086-27-68754067.

Email: geraldchan@whu.edu.cn;

Reagents and instruments

Doxorubicin hydrochloride were obtained from Sangon Biotech (Shanghai). AZ 9260 photoresists were purchased from AZ Electronic Materials (USA). Negative photoresist SU-8 and the developer were purchased from MicroChem Corp. (USA). Indium tin oxide (ITO) glasses were purchased from LaiBao (LaiBao Hi-Tech Co., Ltd., China). PDMS and curing agent were obtained from GE Toshiba Silicones Co., Ltd., Japan. N-(3-Dimethylaminopropyl)-N'-ethylcarbodiimide hydrochloride (EDC), N-hydroxysuccinimide (NHS), Hoechst 33342, bovine serum albumin (BSA), Calcein-AM and propidium iodide (PI) were purchased from Sigma-Aldrich. The collagen solution (rat tail collagen type I) was purchased from Corning (USA). Streptavidin was purchased from Amresco (USA). DNase I was purchased from Beyotime Biotechnology. Ultrapure water (18.2 MΩ·cm) was obtained from a Millipore Milli-Q system.

Breast cancer MCF-7 cell, liver cancer Hep G2 cell, human tongue squamous cell carcinoma CAL 27 cell, human peripheral blood leukemia Jurkat T cell and embryonic kidney cell line HEK-293T were purchased from China Type Culture Collection. All the media for cell culture were bought from PAN biotech and Gibco.

An inverted fluorescence microscope (TE2000-U, Nikon, Japan) equipped with a CCD camera (Nikon DS-Ri1) was used to obtain microscopy images. The fluorescence intensity in chip or solution was monitored by optical fiber spectrometer (QE65000, Ocean Optics, USA). UV-Vis absorption spectra were measured by UV-Vis spectrophotometer (UV-2550, Shimadzu Corporation). Hydrodynamic size and zeta potential were measured by Zetasizer Nano ZS instrument (Malvern). Confocal imaging was used by UltraVIEW VoX (PerkinElmer).

All the HPLC-purified DNA sequences were obtained from Sangon Biotech (Shanghai). And the DNA were individually heated at 95 °C for 5 min and cooled immediately on ice for 10 min, and then left at room temperature for 2 h before used.

Table S1. Sequences of oligonucleotides in this work

Name	Sequences (5′–3′)
Aptamer[1]	5'-**CACTACAGAGGT**TGCGTCTGTCCCACGTTGTCATGGGGGG TTGGCCTGTTTTTTTTT-Biotin-3'
cDNA	5'-**ACCTCTGTAGTG**CCCA**GGCTAGCTACAACGA**CTCTCTCC -3'
S	5'-TGCTGCTGCTGCTGCTGCACCTCGTTTGGAGAGAGrA·rUGG GCACTTTTTTT-Biotin-3'
H1	5'-CGAGGTGCAGCAGCAGCAGCAGCACAAAGTTGCTGCTGCT GCTGCTGC-3'
H2	5'-TGCTGCTGCTGCTGCTGCACCTCGGCAGCAGCAGCAGCAG CAACTTTG -3'

FAM (6-carboxyfluorescein) was labeled at the 5′-end of aptamer and S, Texas Red, BHQ1 (Dark Quencher) were labeled at the 5′-end of cDNA, if necessary. The bold sequences in aptamer and cDNA are complementary. The green sequences in cDNA are the catalytic core of DNAzyme, and underline sequences are recognition arms between cDNA and S. The green sequences in S are cleavage point of DNAzyme. The red sequences in S are the trigger of HCR.

S1 Fabrication of the Microfluidic Devices

Cell captured and drug loading chip: The microfluidic channel was fabricated using the standard soft photolithography method. Briefly, SU-8 2050 photoresist was spin on a silicon wafer and

then exposing it under UV with a mask. After developing and baking in 160 ℃ for 30 min, the PDMS prepolymer mixture (10:1 w/w ratio of oligomer to curing agent) were poured onto the master and dried in 75 ℃ for 4 h. PDMS mold was obtained and punched for inlet and outlet. The fabrication procedure of the nickel patterns was according to our previous work.[2, 3] The prepared nickel patterns were firstly spin coated a thin PDMS film, and together with the PDMS channel were treated by oxygen plasma and bound together to form the microfluidic chip (Fig. S1).

Cell culture chip: The cell-cultured chip has three layers, as shown in Fig. S2. The top and middle layer microchannels were fabricated using the standard soft photolithography method as mentioned above. The difference is that the middle layer was obtained by spin coated a PDMS film, while the top layer was poured the PDMS. Firstly, the middle layer was punched the four cell culture chambers, and bound with the top layer, which was also was punched the outlet before. After binding the top and middle layer, they were punched the inlet, and bound with a clean cover glass (Fig. S2c).

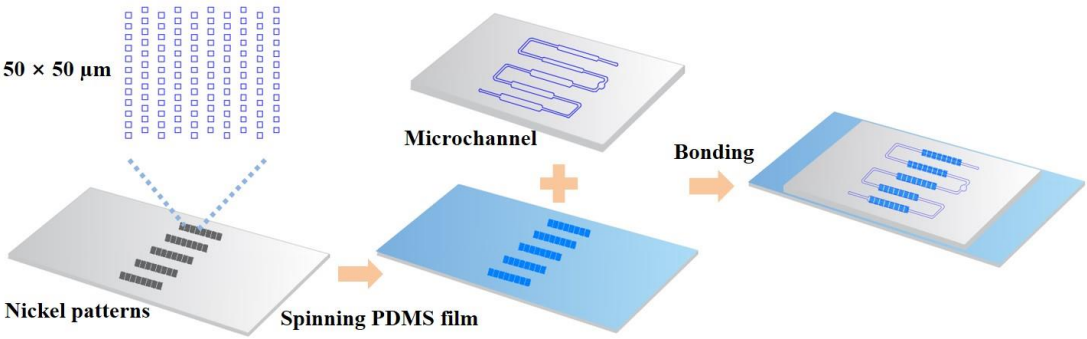

Fig. S1 Design and fabrication of the cell captured and drug loading chip. The nickel patterns were consisted of 50 × 50 μm rectangles, and then were spin coated a thin PDMS film, and bound with the microchannel to form the microfluidic chip.

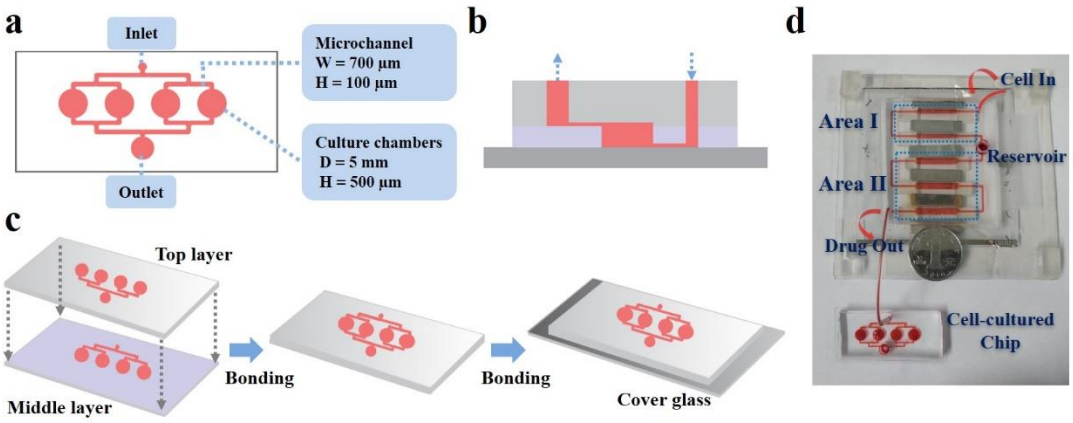

Fig. S2 Design and fabrication of the cell culture chip. (a) The structure chart of the cell culture chip. The size of the cell culture chambers is 5 mm (diameter: D) ×500 μm (height: H), and the microchannels are 700 μm (width: W) ×100 μm (height: H). (b) Cross-section view of the cell culture chip. (c) The fabrication process of the cell culture chip. (d) Photograph of the microfluidic chips, with explanation.

S2 Characterization of MNs-apt-cDNA

The microscopic images in the Fig. S3 are show the cDNAs were successfully hybridized, which was illustrated the fabrication of MNs-apt-cDNA. Meanwhile, the hydrodynamic size and zeta potential of the MNs-SA, MNs-apt and MNs-apt-cDNA were measured. As shown in Table S2, the hydrodynamic size of MNs increased with the aptamers modified (from 447.0 nm to 453.8 nm) and cDNAs hybridized (from 453.8 nm to 467.6 nm). The zeta potential of MNs became more negative due to the DNA modified (Table S2). These results show the successfully fabrication of MNs-apt-cDNA.

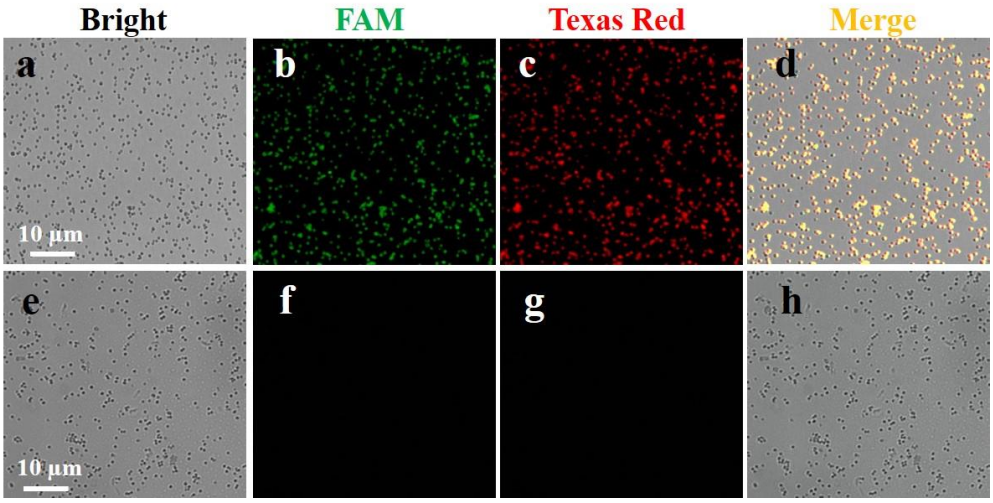

Fig. S3 Microscopic images of the MNs-SA modified with aptamer and cDNA. Bright image, fluorescence image and merge of the images of the MNs-SA (a, b, c, d) and MNs (e, f, g, h) after reacted with FAM-labeled aptamer and Texas Red-labeled cDNA.

Table S2. Hydrodynamic size and zeta potential of the MNs-SA, MNs-apt and MNs-apt-cDNA

Name	Size (nm)	PDI	Zeta Potential (mV)
MNs-SA	447.0	0.026	-19.9
MNs-apt	453.8	0.065	-35.5
MNs-apt-cDNA	467.6	0.037	-45.6

S3 Confocal imaging of tumor cells with aptamers

FAM-labeled aptamers (200 nM) were incubated with the MCF-7 cells and HEK-293T cells in binding buffer at 4 ℃ for 60 min in the dark. After that the cells were washed twice with washing buffer. For confocal imaging, FAM was excited with the laser of 488 nm, and the emission filter was selected 525 nm (W50). In the results (Fig. S4), the MCF-7 cells show high fluorescence signals, while the

EpCAM-negative cell line HEK-293T show no obvious fluorescence signal. The results confirmed that the aptamer can selectively bind the EpCAM-positive cell lines but not the negative cells.

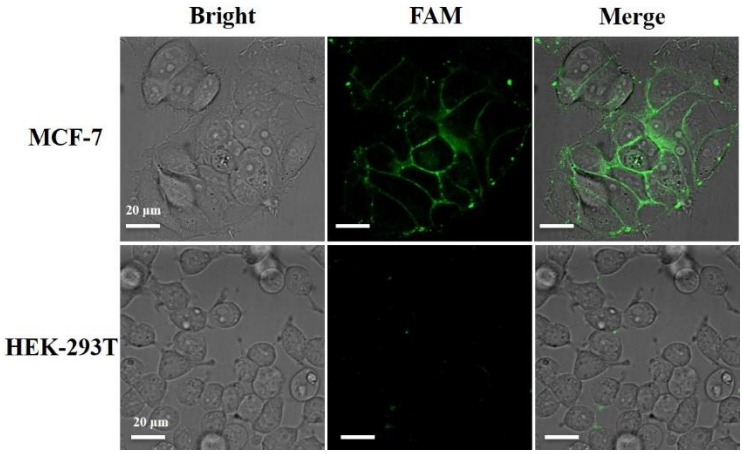

Fig. S4 Confocal images of the MCF-7, HEK-293T cells stained with the FAM-labeled aptamer.

S4 Native polyacrylamide gel electrophoresis (PAGE)

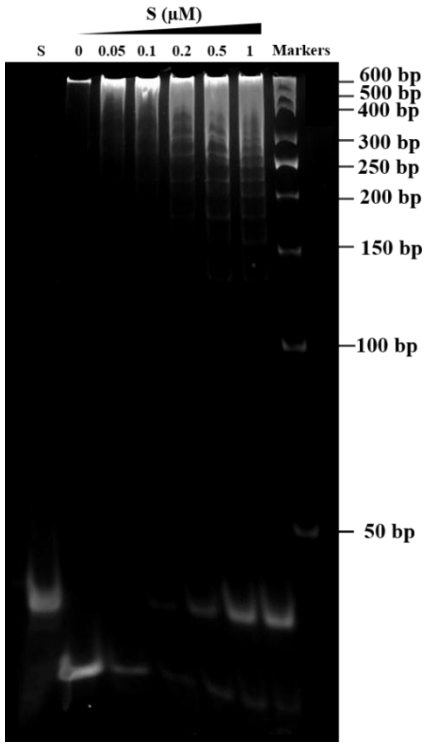

Fig. S5 Native polyacrylamide gel electrophoresis (PAGE) verified the hybridization chain reaction (HCR). 5% PAGE gel was used to analyzed the sample, the gel was stained with Gel Red before imaging. Lane 1: trigger (S: 1 μM), Lane 2-7: a series of increasing concentrations of trigger (S: 0–1 μM) were added to mixtures of H1 and H2 (1 μM each), Lane 8: Markers.

S5 Construction and Characterization of MNs-DOX-DNTs

The drug loading process is shown in the Fig. S6, the hydrodynamic size and zeta potential of the MNs-SA and MNs-DOX-DNTs were measured by DLS (Table S3). The hydrodynamic size of MNs-SA increased to 1336 nm when DOX-DNTs were immobilized on the surface of MNs-SA, and the zeta potential of MNs-SA became more negative, demonstrating the fabrication of MNs-DOX-DNTs.

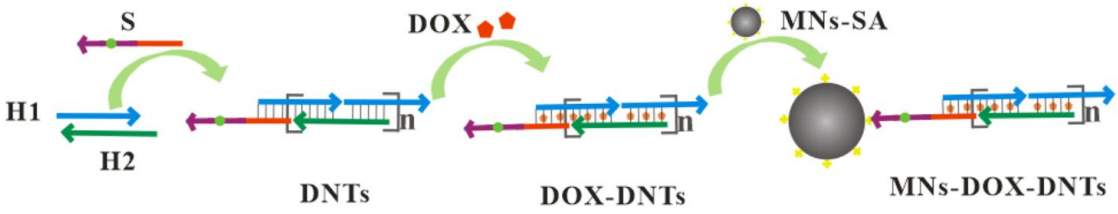

Fig. S6 Schematic diagram of drugs loading process.

Table S3. Hydrodynamic size and zeta potential of the MNs-SA and MNs-DOX-DNTs

Name	Size (nm)	PDI	Zeta Potential (mV)
MNs-SA	450.1	0.042	-17.5
MNs-DOX-DNTs	1336	0.161	-44.1

S6 Cell captured and induced drug released

MCF-7 cells were captured by MNs-apt-cDNA patterns in the chip (Fig. S7a). The effect of flow rate on cell capture efficiency of MNs-apt-cDNA patterns was investigated. As show in Fig. S7b, the capture efficiencies decreased as the flow rate increased. The capture efficiencies were > 85% at the flow rate of 1.5 μL min^{-1} (87.4% ± 3.7%) and 2 μL min^{-1} (85.5% ± 1.0%). Thus, the flow rate of 2 μL min^{-1} was selected for the cell capture experiments to obtain higher flux.

The released drugs were in the form of complexes, and there was no fluorescence of DOX until the drugs entered the cells (or DNase I treated, Fig. S7b) and expressed fluorescence by unloading the DOX.

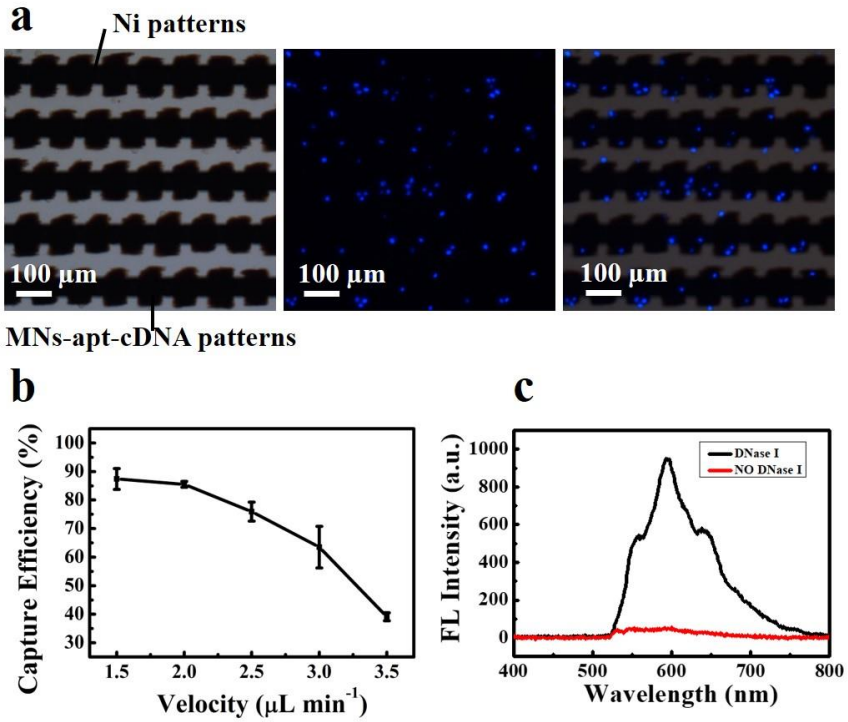

Fig. S7 (a) Microscopic images of the MCF-7 captured in chip by MNs-apt-cDNA patterns. Cells nuclear were stained by Hoechst 33342. (b) The effect of flow rate on cell capture efficiency of

MNs-apt-cDNA patterns. (c) The fluorescence of DOX when used DNase I treated and not used DNase I treated.

S7 Cell cultured in microfluidic chip

The growth of MCF-7 cells in the chip was observed by microscopic imaging at 12, 24, 36, 48, 60 h. Calcein-AM and PI were used to stain the cells at 60 h. As shown in Fig. S8a, the cells grow well and cover the bottom at 60 h. The viability of cells was no obvious difference compare to the well plates (Fig. S8b).

In vitro three-dimensional cell culture was more suitable to mimic the extracellular matrix (ECM) comparing with traditional two-dimensional cell culture.[4] Tumor cell spheroids in the collagen gel were used to simulate the solid tumors. Because of the good biocompatibility and special structural properties, collagen can effectively simulate ECM and achieve three-dimensional culture of cells. The growth of tumor cell spheroids was observed under microscope. The cell spheroids were stained by Calcein-AM and PI at day 14. The results in Fig. S9 show that the cell spheroids grew well and kept good viability in two weeks.

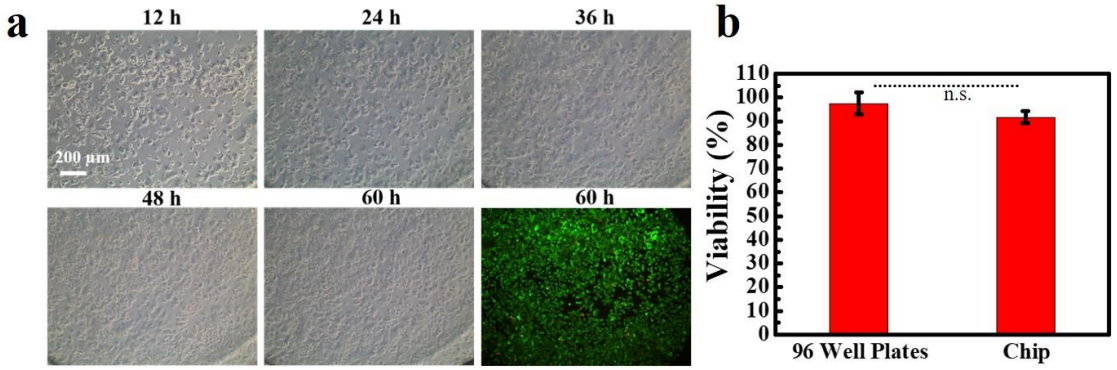

Fig. S8 Cell cultured in microfluidic chip. (a) Microscopic images of the cells cultured in microfluidic chip at 12, 24, 36, 48, 60 h. Calcein-AM and PI stained the cells at 60 h. Scale Bar: 200 μm. (b) The viability of the cells that cultured in microfluidic chip compare to the 96 well plates (n.s., not significant, $P > 0.05$, $n = 3$).

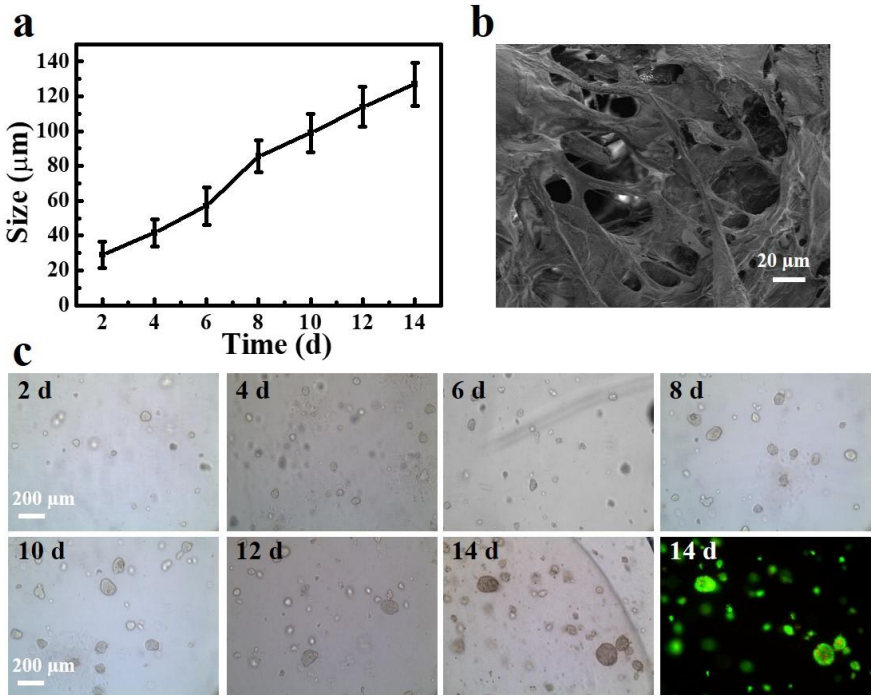

Fig. S9 (a) The change of the spheroids size during the cultured process. (b) SEM micrographs of collagen with a concentration of 2.5 mg mL^{-1}. (c)Microscopic images of the cell spheroids cultured in microfluidic chip at 2, 4, 6, 8, 10, 12, 14 day. Calcein-AM and PI stained the cell spheroids at 14 day.

S8 Confocal imaging of tumor cell spheroids

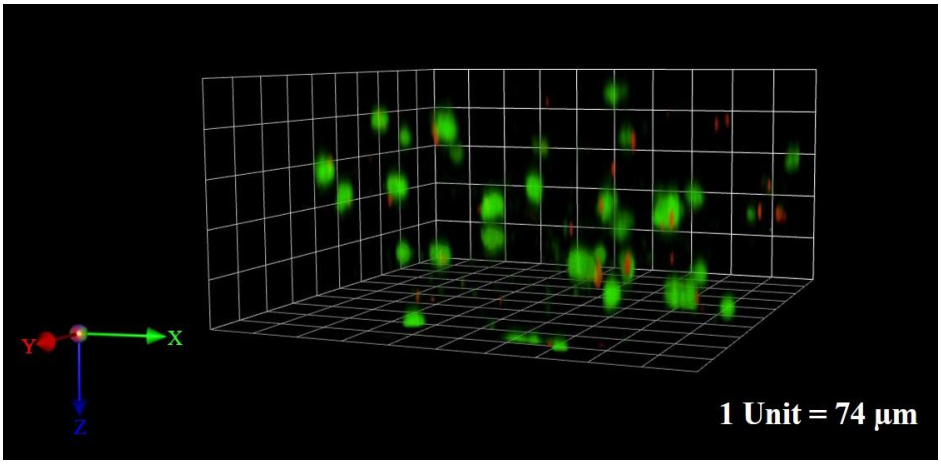

Fig. S10 Z-stacked scanning confocal image of cell spheroids cultured in the collagen at microfluidic chamber. The scanned height was 400 µm and the z spacing was 4 µm. The cell spheroids were stained by Calcein-AM and PI.

References

1 Y. Song, Z. Zhu, Y. An, W. Zhang, H. Zhang, D. Liu, C. Yu, W. Duan and C. J. Yang, *Anal. Chem.*, 2013, **85**, 4141-4149.

2 X. Yu, X. Feng, J. Hu, Z. L. Zhang and D. W. Pang, *Langmuir*, 2011, **27**, 5147-5156.

3 M. Tang, C. Y. Wen, L. L. Wu, S. L. Hong, J. Hu, C. M. Xu, D. W. Pang and Z. L. Zhang, *Lab on a chip*, 2016, **16**, 1214-1223.

4 X. Du, W. Li, G. Du, H. Cho, M. Yu, Q. Fang, L. P. Lee and J. Fang, *Anal. Chem.*, 2018, **90**, 3253-3261.